GEOLOGIJA *53/2*, 129–138, Ljubljana 2010
https://doi.org/10.5474/geologija.2010.010

Mineral chemistry of polymetallic mineralization associated with altered granite, Hangaliya area, South Eastern Desert, Egypt

Mohamed F. RASLAN & Mohamed A. ALI
Nuclear Materials Authority. P. O. Box 530, El-Maadi, Cairo, Egypt;
e-mail: raslangains@hotmail.com

Prejeto / Received 13. 4. 2010; Sprejeto / Accepted 30. 9. 2010

Key words: polymetallic mineralization, altered granites, quartz veins, Hangaliya gold deposit, Egypt

Abstract

The Hangaliya gold deposit, located in the South Eastern Desert of Egypt, comprises a series of milky quartz veins along NW-trending Hangaliya shear zone, cutting through granitic rocks of Gabal Nugrus monzogranite. This shear zone, along with a system of discrete shear and fault zones, formed in the late deformation history of the area. The quartz vein emplacement took place under a brittle-ductile shear regime. Auriferous quartz veins are slightly sheared and boudinaged within the shear zone, especially in the hematized granite. Hydrothermal alteration is pervasive in the granitic wall rocks including sericitization, chloritization, fluoritization, sulphidization and minor carbonatization. The altered zones and associating quartz veins contain sulphides, gold, silver, cobalt, bismuth, and uraninite minerals.

The Hangaliya gold veins include gold, silver, cobaltite, native bismuth, chalcopyrite, pyrite, galena, ferrocolumbite, fergusonite and uraninite. The Au-ore occurs in the quartz veins and adjacent wall rocks as dissemination in chalcopyrite and pyrite. Presence of refractory native silver, bismuth and cobalt in chalcopyrite is inferred from microprobe analyses. Wall rock sulphidization also likely contributed to destabilising the gold-silver, cobalt, bismuth assemblages and precipitation of the minerals in the hydrothermal alteration zone adjacent to the quartz veins. Gold occurs in two main modes: "invisible gold" in sulphides and native gold. Most of the "invisible gold" occurs in chalcopyrite and bismuth. The altered granites in the Hangaliya shear zone are enriched in Au, Ag, Bi, Co, and Ni with chalcopyrite, which suggests derivation of these metals from serpentinites due to interaction with the felsic Nugrus granite.

Introduction

The Eastern Desert of Egypt has long been a mining district for gold, with more than 95 gold occurrences mostly confined to the Neoproterozoic basement rocks (El Ramely et al., 1970; Abdel Tawab, 1992; Takla, 2001). Mining activity was extensive during the Pharaonic and Roman times and exploitation of the major gold deposits, e.g. El Sid, El Barramiya and El Sukari, continued until 1958 (Sabet & Bordonosov, 1984). In most of the gold occurrences in the Eastern Desert of Egypt, gold occurs in the hydrothermal quatrz veins cutting through basement rocks of different compositions including metavolcanics, schists, serpentinite and granitoids. Mineralogy of these veins commonly includes fine dissemination of native gold, As-bearing pyrite, arsenopyrite and chalcopyrite together with subordinate sphalerite, galena, tetrahedrite and stibnite (Azer, 1966). They are interpreted collectively as products of hydrothermal activity (Garson & Shalaby, 1976) induced either by metamorphism or cooling of Early Palaeozoic magmatic rocks (Almond et al., 1984) or subduction-related younger calc-alkaline magmatic rocks (El-Gaby et al., 1988). Other authors relate gold mineralization to the emplacement of granitoid rocks that intrude mafic/ultramafic rocks (El Shazly, 1957). Gold was deposited at 300–400 °C and 1–2 kbar (Klemm et al., 2001), the conclusion supported by Harraz (2000, 2002) for the deposits at the El-Sid and Atud mines, in the Central Eastern Desert. Almond et al. (1984) suggested that gold deposition was linked to an episode of shearing post-dating the emplacement of all batholithic intrusions and coeval with regional cooling. On the other hand, Hussein (1990) argued that most of these hydrothermal vein deposits were epithermal rather than mesothermal. In all cases, gold is considered to have been leached either from metabasaltic or ultramafic rocks through the circulation of metamorphic or mixed metamorphic-magmatic fluids (e.g. Hassaan & El-Mezayen, 1995; Harraz, 2000; Klemm et al., 2001; Botros, 2004).

The old Hangaliya gold deposit is a typical example of a deposit formed in vicinty of granites. Hume (1937) mentioned that gold-bearing quartz veins at Hangaliya mine are associated with sericitzation and silicification at the vein

contacts with the Nugrus granites. This was also observed by SOLIMAN (1986) who also added that the relative enrichment of the Nugrus granites in Sn at the Hangaliya deposit area is ascribed to its derivation from stanniferous S-type granitic magmas formed by partial melting of metasediments.

Mode of occurrence and genesis of gold at Hangaliya were subjects of studies by some authors. OSMAN and DARDIR (1986, 1989) showed that gold mineralization at Hangaliya occurs in simple fissure-filling quartz veins in the WNW-ESE trending sheared Nugrus granite. They recorded pronounced greisenization, chloritization, sericitization in addition to kaolinitization and ferrugination. Pyrite and native gold are common in the quartz veins of Hangaliya (OSMAN, 1989). KHALIL and HELBA (1998) showed the relation between gold mineralization at Hangaliya and the interaction of the granites with the ultramafic and metagabbro-diorite rocks association. SUROUR et al. (1999) studied in detail the microfabrics of this shear zone in the vicinty of the old gold mine of Hangaliya and concluded that conjugate fracture system and formation of mega- and microscopic porphyroclasts in the sheared granites are the most common features of the shear sense. Abundant gold (up to 3.3 ppm) in the shear zone is evidenced by the presence of microscopic native gold. SUROUR et al. (2001) showed that the source of gold is multiple, being leached from the ophiolitic serpentinites, arc-metavolcanics and sulphide-bearing dolerite dykes. Also, they reported that the rock varieties in the auriferous shear zones in the granite are enriched in Cr and Co, which suggests transfer of these metals from serpentinites due to the interaction with the felsic Nugrus granite, which is also enriched in U. The present paper presents mineral chemistry and mineralogy of the noble elements and minerals associated with the auriferous shear zones at Hangaliya deposit. Also, the source of Au, Ag, Bi, Co, Ni and U in the shear zones and adjacent country rocks is discussed.

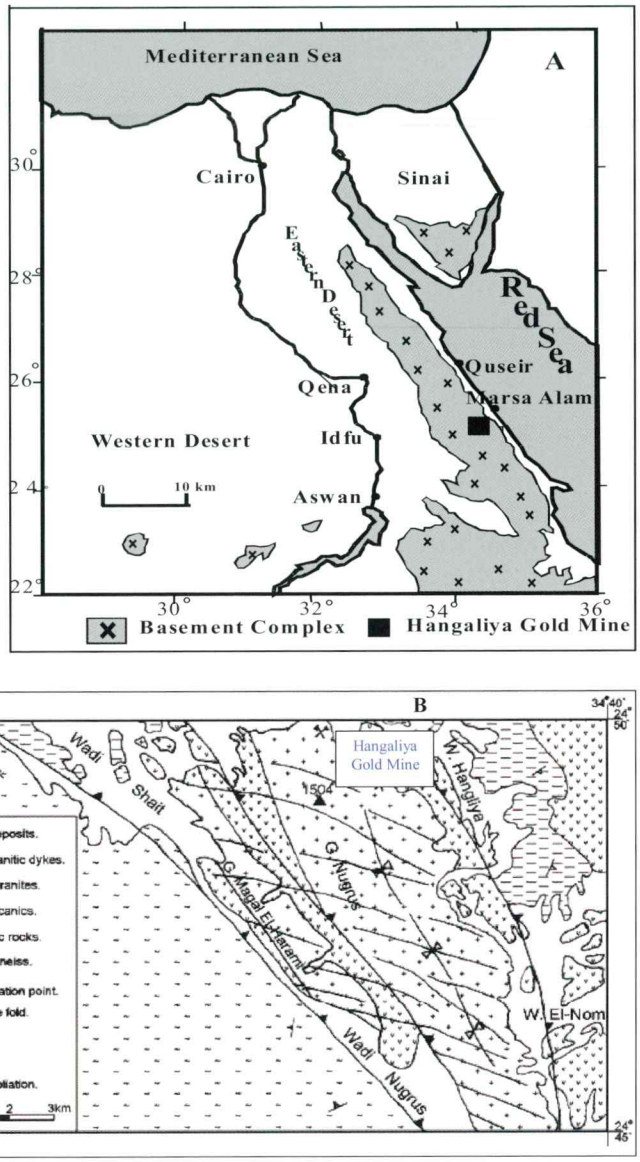

Fig. 1. A – Location map of the study area, B – Geological map of Gabal Nugrus monzogranite and location of the Hangaliya Gold mine (modified after SUROUR et al., 2001)

Geological setting

The Hangaliya gold mine, located in the South Eastern Desert of Egypt (Fig. 1A), comprises a series of milky quartz veins along NW-trending shear zone, cutting through Gabal Nugrus monzogranites. Rocks along the shear zone show different types of hydrothermal alterations such as silicification, hematitization and kaolinitization. The vein emplacement took place under a brittle-ductile shear regime. Auriferous quartz veins are characterized by irregular walls. Hydrothermal alteration is pervasive in the granitic wall-rocks including sericitization, silicification, sulphidization and minor carbonatization. These types of alterations and associating quartz veins contain sulfides, gold, silver, bismuth and U- and Th- minerals.

The younger granites (Gabal Nugrus & Gabal Magal El-Harami) in the studied area are represented by elongated belt trending in NW-SE direction (Fig. 1B). They intrude metavolcanics and contain xenoliths of different sizes and shapes from these rocks. The composition of the younger granites of Gabal Nugrus ranges from monzogranites to syenogranites. They are cut by several microgranitic dyke swarms (EL-HUSSEINY et al., 2006).

A shear zone trending NW-SE, crosscuts the northern segment of Gabal Nugrus (1504 m a.s.l) and extends for 300 meters (Fig. 2A). The identification of the shear zone was based on field obsevations. The younger granites are mylonitized and cataclased within the shear zone. The intensely mineralized part of the shear zone encountered in the monzogranites varies in width from 0.5 to 2.5 meters and in length from 100 to 300 meters. Some auriferous quartz veins occur along or cut the shear zone (Fig. 2B).

Fig. 2. A – Photo shows NW trending shear zone of the Hangaliya Gold mine, South Eastern Desert, Egypt, B – Sketch of the quartz vein cutting the altered granites of the Hangaliya shear zone, South Eastern Desert, Egypt

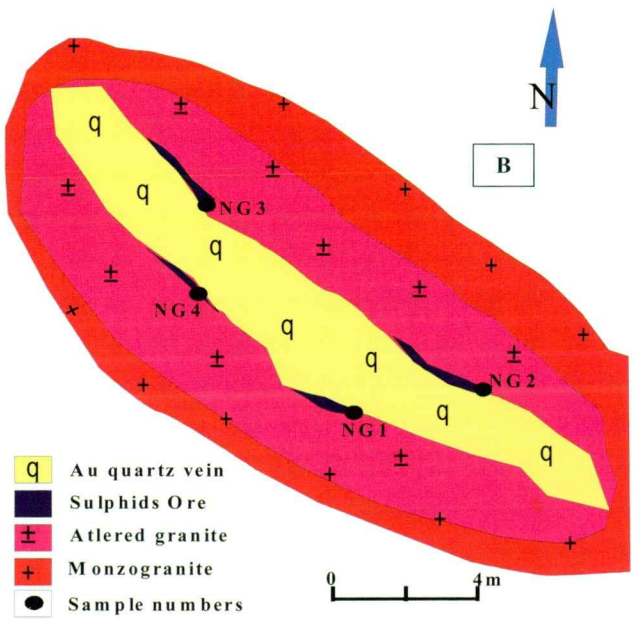

Methodology

About 10 rock specimens were collected from the mineralized shear zone of the Hangaliya gold deposit, from which 8 thin-sections were prepared. The petrographical study was achieved using a polarizing microscope. The study involved the preparation of heavy mineral fractions using heavy liquid separation and magnetic separation. Some of the selected mineral grains were analyzed with the environmental scanning electron microscope (ESEM) supported by energy dispersive spectrometer unit (EDS) model Philips XL 30. The analytical conditions were 25–30 kV accelerating voltages, 1–2 micron beam diameter and 60–120 second counting times. Minimum detectable weight concentration of elements from 0.1 to 1 wt. % was obtained. Precision well below 1 %, the relative accuracy of quantitative results 2–10 % for elements Z>9 (F), and 10–20 % for the light elements B, C, N, O and F.

The analyses were carried out at laboratories of the Egyptian Nuclear Materials Authority (NMA).

Polished thin-sections were studied under reflected light in order to determine mineral associations and parageneses. Backscattered electron images (SEM-BSE) were taken with the scanning electron microscope, coupled with an energy dispersive spectrometer (model JEOL 6400 SEM) at the Microscopy and Microanalyses Facility, University of New Brunswick (UNB), Canada. Mineral compositions were determined with the electron probe microanaylsis (EPMA) JEOL JXA-733 Superprobe. The EPMA accelerating voltage was 15 kV, with a beam current of 50 nA and peak counting times 30 seconds for all elements. Combinations of well characterized natural and synthetic minerals and pure metals were used as standards. Pure metals were used for Cu, Ag, Se, Au, Bi, Co, Ni, Fe, Nb, Ta, Mn, Sn, Th and U. From natural and synthetic minerals we used pyrite for Fe and S; stibnite for Sb, sphalerite for Zn, synthetic GaAs for As; jadeite, quartz and apatite for Na, Si, and P and Ca, respectively; $SrTiO_3$ for Ti, YAG for Y; La-, Ce-, Nd-, Pr- and Gd- Al; Si bearing glass for (La, Ce, Nd, Pr and Gd) and crocoite for Pb. Apparent concentrations were corrected for matrix effects with the PAP correction program.

Mineralogical and geochemical investigation

Optical microscopy study

Petrographically, quartz (35–55 %) sometimes shows clear signs of mylonitization. Alkali feldspars are represented by orthoclase perthite with subordinate microcline. They are penetrated by relatively fine-grained veinlets of quartz and are kaolinitized along the cleavage planes and frac-

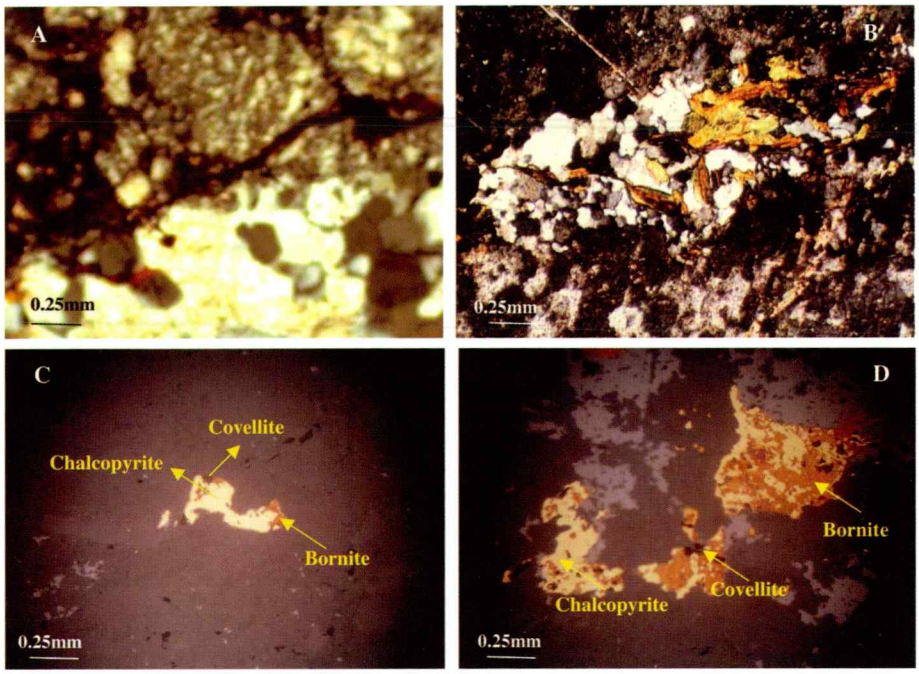

Fig. 3. A – Photomicrograph shows a general view of minerals composition of cataclastic (altered) granites, B – Biotite flakes associated with secondary quartz within altered granites, C – Photomicrograph show chalcopyrite altered to covellite and bornite, D – Large crystal of chalcopyrite that completely altered to bornite and covellite. All photographs in the figure are taken under Crossed Nichols, C.N.

tures. The cracks opened path for the late iron-rich hydrothermal solutions (Fig. 3A), which caused iron staining and gave the rock its red coloration (Fig. 3B). Cataclased albite (5 %) is commonly altered to sericite and the abundance of sericite increases in the mineralized samples. Due to cataclasis the grains are microfractured and twin lamellae are bent. Iron oxides occur in all studied sections either as a primary or as a secondary phase resulting from the alteration of other primary minerals, which are completely replaced by hematite. Locally, the original composition of the granites is obscured by the high intensity of hematitization and pyritization. Chalcopyrite occurs as euhedral to subhedral grains. Chalcopyrite is completely altered to bornite and covellite (Figs. 3C, D).

Environmental scanning electron microscope and energy dispersive spectroscopy (ESEM/EDS) study

Native gold was detected microscopically in the mineralized samples. Most of gold particles are generally in a form of aggregates, of scally habit and very malleable and ductile. They have high reflectivity and brilliant luster (Fig. 4A). From some of the selected gold flakes three semiquantitative analyses using the (ESEM/EDS) were made. The obtained two semiquantitative analyses for gold (Figs. 4B, C, D) show Au as the essential component ranging from 66.6 to 78 wt.% with an average of 70.7 wt.%. Beside, significant amount of Ag ranging from 19.6 to 32.3 % with an average of 27.9 % and minor amount of Fe ranging from 0.7 to 2.4 % with an average of 1.4 % were found. The chemical composition of the separated pyrite crystals was analyzed by ESEM/EDS (Figs. 4E, F, G). The major elements in these crystals are S (51.3 %) and Fe (43.3 %) together with minor amounts of Si (2.7 %) and Zn (1.7 %). Galena occurs as inclusions within pyrite crystals as indicated from ESEM/EDS analyses (Figs. 4F, H). The obtained spectra of these inclusions gave Pb (66.4 %) and S (22.8 %) as essential components together with minor Si and Fe. The EDS analysis (Fig. 4I) reflects the chemical composition of chalcopyrite crystals where the major elements are Cu (53.7 %), S (24 %) and Fe (10.7 %). Cobaltite crystals occur as inclusions in pyrite. Two semiquantitative analyses of cobaltite (Fig. 4J) yielded Co (12.8–10.4 %) with an average of 11.6 %, As (30.5–23.8 %) with an average of 27.2 % and S (17.7–15.7 %) with an average of 16.7 %. Significant amounts of Ni, Cu, Fe, Si and Al were also detected.

Electron probe microanalyses

Invisible and native gold (Au)

EPMA analyses indicated that the gold content in the studied chalcopyrite and native bismuth attains 300 and 313 ppm respectively. While average "invisible gold" can attain 240 ppm in cobaltite, it can reach 250 ppm in native Ag associated with chalcopyrite. Sulphides are actually the principal Au-bearing minerals in refractory gold ores where gold is often referred to as "invisible" gold. Recent spectroscopic and high-resolution electron imaging studies have revealed that the invisible gold occurs within the structure of pyrite and, to a lesser extent, as submicroscopic or nanoparticles of native gold (Simon et al., 1999; Palenik et al., 2004; Reich et al., 2005; Paktunc et al., 2006). The obtained data revealed that the detected gold in the studied minerals is present mainly as "invisible gold" rather than as submicroscopic or nanoparticles of native gold and occurs within the structure of chalcopyrite most probably incorporated as chemically bonded gold. Cepedal et al. (2008) favor a mechanism in which "invisible gold"

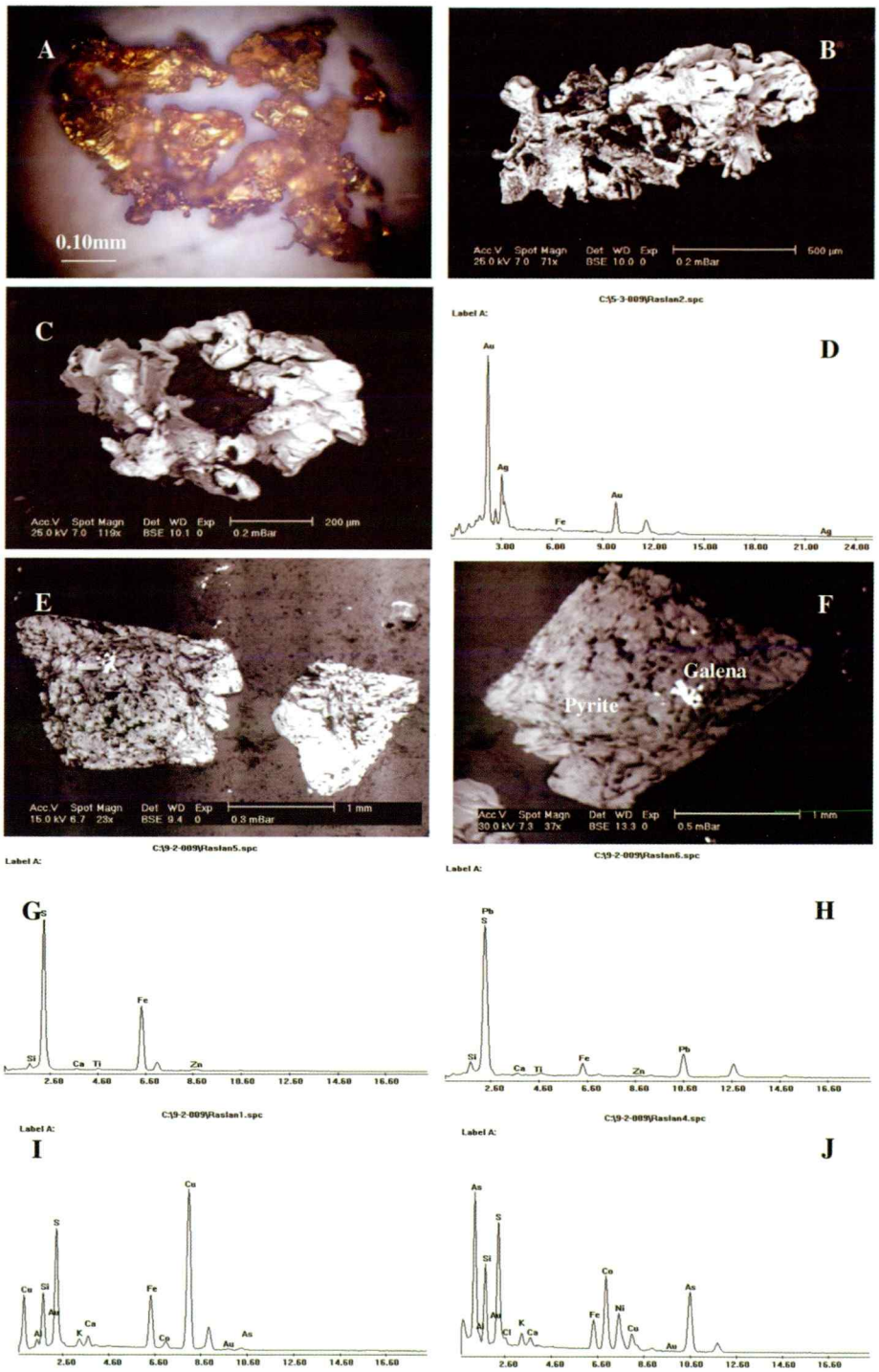

Fig. 4. A – Native gold with aggregate-like structure (Binouicular microscope), B & C – Backscattered electron images illustrating the native gold aggregates, D – EDS spectrum of gold, E – SEM-BSE image of pyrite containing galena inclusions, F – SEM-BSE image of galena inclusion in pyrite, G, H, I & J – EDS spectra of pyrite, galena, chalcopyrite and cobaltite, respectively.

was removed from ore fluids by chemisorption at As-rich, Fe-deficient surface sites in As-rich pyrite and arsenopyrite and incorporated into the sulphides as solid solution. This process took place during sulphidization of the host rocks.

Native bismuth (Bi)

Bismuth occurs as numerous subhedral to anhedral crystals within chalcopyrite with size ranging from 0.5 to 3 μm (Fig. 5A). The EPMA analyses of these inclusions reflect the chemical composition of native bismuth. The major element is Bi (93.6 %) together with elemental composition of chalcopyrite ($CuFeS_2$=6.4 %). The bismuth-nickel association is found with composition of Bi (62.7 %) and Ni (25.5 %) in chalcopyrite ($CuFeS_2$=14.2 %) (Table 1; Fig. 5A).

Chalcopyrite ($CuFeS_2$)

Chalcopyrite occurs as subhedral to euhedral crystals ranging in size from 50 to 200 μm (Fig. 5A, B). The EPMA analyses of the chalcopyrite reflect its chemical composition and gave [S (34–35 %), Fe (29–31 %), and Cu (29–34 %)], together with minor Bi, Ni, Co and Ag (Table 1; Fig. 5A, B).

Native silver (Ag)

Native silver (Ag) occurs as inclusions within the chalcopyrite and formed mainly from the hy-

Elements wt %	Chalco-pyrite 4N2	Chalco-pyrite 6N2	Chalco-pyrite 8N2	Chalco-pyrite 5N2	Bi-Ni in Chalco-pyrite 2N2	Native-Bi 3N2	Native-Bi 4N2
S	34.97	34.22	35.15	34.41	10.41	1.602	1.493
Fe	30.76	28.93	30.45	29.41	1.767	1.5367	1.433
Cu	34.16	28.54	33.65	31.88	1.985	3.62	3.38
As	0.000	1.080	0.194	0.000	0.000	0.000	0.000
Co	0.043	1.946	0.593	0.028	0.010	0.034	0.036
Ni	0.042	1.016	0.122	0.000	25.51	0.002	0.002
Bi	0.125	0.712	0.099	0.070	62.74	93.17	93.63
Ag	0.000	0.295	0.053	1.095	0.021	0.000	0.000
Au	0.000	0.000	0.030	0.000	0.000	0.032	0.030
Sb	0.000	0.000	0.000	0.000	0.000	0.000	0.000
Zn	0.000	0.000	0.000	0.000	0.000	0.000	0.000
Se	0.007	0.122	0.003	0.015	0.000	0.000	0.000
Sn	0.013	0.000	0.000	0.000	0.000	0.000	0.000
Pb	0.022	0.100	0.102	0.081	0.000	0.000	0.000
Total	100.14	96.96	100.44	96.99	102.44	100.00	100.02

Table 1. EPMA anaylsis of selected chalcopyrite, Bi-Ni in chalcopyrite and native Bi of Hangaliya shear zone (by wt.%), South Eastern Desert, Egypt

drothermal solutions. These inclusions occur as minute anhedral to subhedral crystals associated with chalcopyrite ranging in size from 1 to 5 μm (Figs. 5C, D). Silver was found only in chalcopyrite of the Hangaliya shear zone as an alteration phase, characterized by very light grey color and is potentially concentrated in the chalcopyrite together with traces of Au; This was obtained by SEM-BSE images and by EPMA chemical analyses. The silver is composed of Ag and Au (Figs. 5C, D; Table 2).

Cobaltite (CoAsS)

Cobaltite occurs as euhedral to subhedral crystals of the Hangaliya shear zone. Cobaltite appears brighter than chalcopyrite under SEM-BSE. The obtained results of EPMA analysis confirm the chemical composition of the studied cobaltite (Fig. 5B; Table 2). The contents of major elements in wt. % are Co (22–27 %), As (45 %), S (19 %) and Ni (6–10 %) (Table 2).

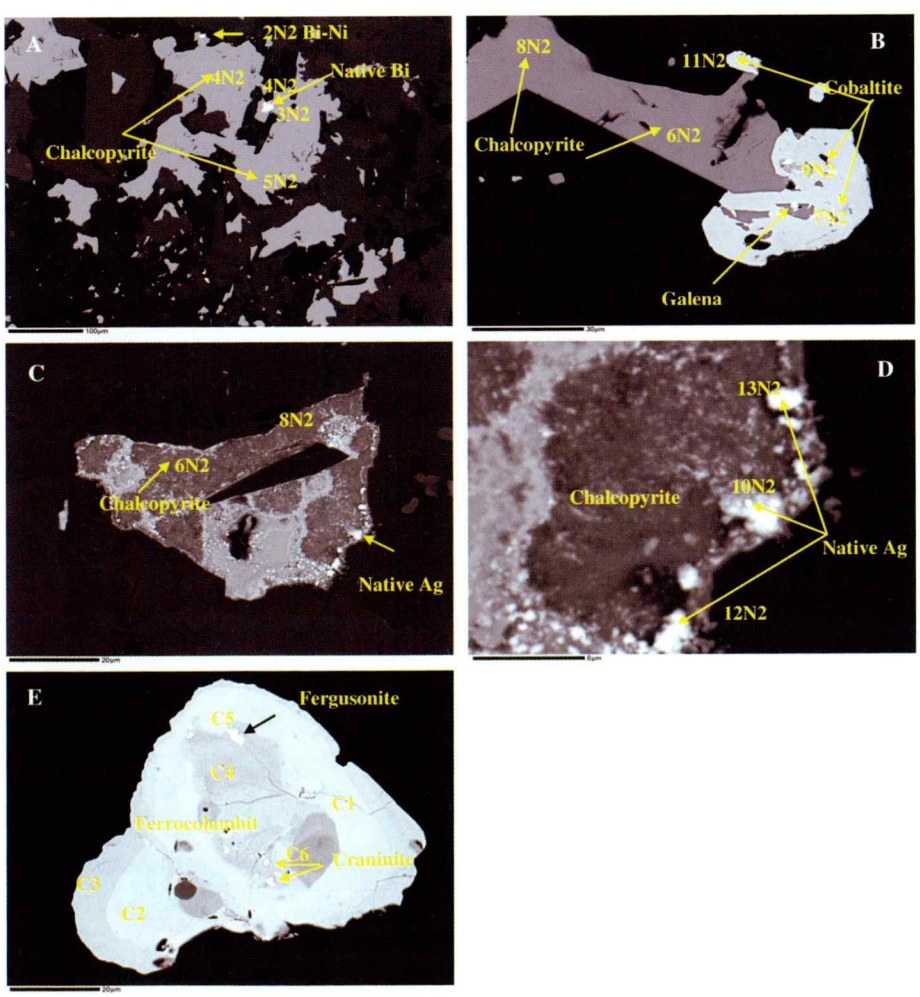

Fig. 5. SEM-BSE images of A – Chalcopyrite rich in native Bi as inclusions B – Chalcopyrite, cobaltite associated with galena as inclusion, D – Chalcopyrite rich in native Ag, C – Large crystal of native silver (Ag) as an inclusion in chalcopyrite, E – Uraninite and fergusonite as inclusions in the ferrocolumbite of the altered granite of Hangaliya mine.

Elements wt %	Cobaltite 7N2	Cobaltite 9N2	Cobaltite 11N2	Native-Ag in chalcopyrite 10N2	Native-Ag in chalcopyrite 12N2	Native-Ag in chalcopyrite 13N2
S	19.43	19.14	19.23	22.37	10.54	6.38
Fe	2.980	3.94	4.00	15.21	37.15	18.97
Cu	0.233	0.251	0.267	38.73	9.81	10.93
As	45.21	45.60	44.99	0.024	0.180	0.023
Co	27.02	21.50	22.92	0.000	0.010	0.070
Ni	5.97	9.77	6.88	0.017	0.180	0.096
Bi	0.074	0.041	0.043	0.131	0.042	0.029
Ag	0.023	0.039	0.000	23.25	41.77	63.33
Au	0.004	0.024	0.002	0.025	0.022	0.025
Sb	0.000	0.012	0.048	0.000	0.000	0.000
Zn	0.000	0.000	0.000	0.000	0.047	0.000
Se	0.163	0.165	0.226	0.000	0.038	0.069
Sn	0.000	0.000	0.000	0.000	0.000	0.000
Pb	0.030	0.028	0.041	0.240	0.226	0.071
Total	101.09	100.51	98.65	100.00	100.06	100.2

Table 2. EPMA anaylsis of selected cobaltite, native Ag of Hangaliya shear zone (by wt.%), South Eastern Desert, Egypt

Galena (PbS)

Galena occurs as numerous inclusions of variable size in chalcopyrite and pyrite crystals (Figs. 4B, E, F).

Pyrite (FeS_2)

Pyrite has well developed octahedron crystals with pale-brass yellow color and metallic luster (Figs. 4E, F). Pyrite is usually disseminated in the altered rocks of the Hangaliya shear zone. Generally, pyrite of the studied shear zone is partly or entirely oxidized to Fe-oxy-hydroxides such as hematite and goethite. This process can be classified as pseudomorphic desulphidization under oxidizing conditions.

Columbite [(Fe, Mn) $(Nb,Ta)O_4$]

The columbite group of minerals comprises a large number of structurally related orthorombic AB_2O_6 compounds (B= Ta, Nb). The columbite subgroup is Nb-dominant, and the tantalite subgroup is Ta-dominant. They contain U (and Th) in various amounts and are commonly metamict but none has been described with U as essential constituent. The relatively small octahedral A-site is commonly occupied by Mg^{2+} (magnesiocolumbite) and transition-metal cations such as Fe^{2+} (ferrocolumbite) and Mn^{2+} (manganocolumbite), while U and Th substitutions are relatively minor. Columbite that occurs in the altered rocks of the shear zone at Hangaliya area generally forms subhedral to anhedral (Fig. 5E). EPMA analyses of columbite crystals are presented in Table 3. The obtained results indicate that the chemical com-

Sample	NUG-N8	NUG-N8	NUG-N8	NUG-N8	NUG-N8	NUG-N8
Mineral	Ferro columbite (light) C1	Ferro columbite (light) C2	Ferro columbite (dark) C3	Ferro columbite (dark) C4	Fergusonite C5	Uraninite C6
Na_2O	0.087	0.085	0.036	0.036	0.004	0.046
SiO_2	0.000	0.000	0.000	0.000	0.000	0.055
P_2O_5	0.009	0.009	0.010	0.010	0.048	0.003
CaO	0.018	0.017	0.007	0.006	0.552	0.000
TiO_2	0.674	0.6635	0.239	0.235	0.930	0.115
MnO	3.78	3.72	4.11	4.03	0.000	0.515
FeO	16.39	16.13	16.66	16.37	8.192	2.203
Y_2O_3	0.039	0.039	0.242	0.238	18.10	0.277
Nb_2O_5	66.45	65.39	77.12	75.79	51.20	8.86
SnO_2	0.127	0.1246	0.126	0.124	0.000	0.000
La_2O_3	0.000	0.000	0.190	0.187	0.000	0.001
Ce_2O_3	0.143	0.141	0.000	0.000	0.151	0.340
Pr_2O_3	0.041	0.0399	0.000	0.000	0.000	0.000
Nd_2O_3	0.000	0.000	0.000	0.000	0.290	0.000
Gd_2O_3	0.000	0.000	0.000	0.000	0.000	0.300
Ta_2O_5	13.81	13.59	2.963	2.912	0.430	1.515
PbO	0.000	0.000	0.012	0.010	0.978	4.93
ThO_2	0.056	0.055	0.051	0.045	7.20	3.15
UO_2	0.210	0.187	1.412	1.18	11.03	77.63
Total	101.83	100.19	102.27	101.19	99.77	99.64

Table 3. EPMA anaylsis of selected columbite, uraninite and fergusonite minerals in the Hangaliya shear zone, South Eastern Desert, Egypt.

position of the studied columbite crystals are ferrocolumbite. The major elements are Nb, Fe, Ta, and Mn. The EPMA analysis of the ferrocolumbite grain (Fig. 5E) showed that the composition in the light and dark parts (C1, C2 and C3, C4) ranges between 65–77 % for Nb_2O_5, 3–14 % for Ta_2O_5, 16–17 % for FeO and 3–7 % for MnO. Minor and trace contents of SnO_2, UO_2, ThO_2 and PbO were also measures (Table 3).

Fergusonite [(Y, REE>Ca,U,Th)(Nb,Ta)O_4]

The fergusonite group consists of REE-bearing Nb and Ta oxides, many of which are metamict and therefore commonly poorly characterized. Most of these minerals are monoclinic, although orthorhombic and tetragonal unit cells arise from cation ordering. Fergusonite occurs only in the altered granite shear zone of Hangaliya as light grey inclusion in the ferrocolumbite, which contains high concentrations of the Y, U, Th and Ca. The obtained EPMA chemical analyses and SEM-BSE images indicate that this fergusonite phase is predominantly composed of Y, Nb, Ta and U (Fig. 5E; Table 3).

Uraninite (UO_2)

Uraninite is a common accessory mineral in pegmatites and peraluminous granites, and is probably the most important source of dissolved U in groundwaters emanating from weathered granite terrains (Frondel, 1958; Förster, 1999). The uraninite (UO_2) occurs as primary U-mineral in the Ghadir shear zone and is formed during reduction reaction. It is found as minute euhedral crystals ranging from 1–3 μm in size (Fig. 5E). Uraninite crystals appear very bright under scanning electron microscope compared to other uranium minerals. The EPMA analyses of these crystals confirm the chemical composition of uraninite (Table 3). These results indicate that the major oxides in uraninite are [UO_2 (77.6 %), ThO_2 (3.15 %), and PbO (4.9 %), Nb_2O_5 (8.9 %), FeO (2.2 %) and Ta_2O_5 (1.5 %)]. Also, minor amounts of REE and Y were reported as substitutions in uraninite (Table 3).

Discussion

Pyrite occurs with chalcopyrite as euhedral to subhedral interstitial grains. Massive aggregates of chalcopyrite dominate, and commonly have a thin (100 μm) rim of bornite. Locally, covellite replaces bornite along fractures, but also occurs as euhedral grains rimming chalcopyrite. Associated with sulphides at Hangaliya gold deposits, native and invisibile gold were observed in the studied samples of hydrothermally altered zone.

Three types of uraninite can be roughly defined in terms of their genesis (McMillan, 1978); 1 – Igneous, magmatic and metamorphic, including pegmatitic uraninite; 2 – Hydrothermal (e.g. vein type and unconformity-related deposits); 3 – Low temperature (sedimentary-hosted deposits). The chemistry of unaltered uraninite is a reliable indicator of its origin (Frondel, 1958; Förster, 1999). Magmatic uraninite commonly contains Th and REE, whereas these elements are mostly absent from hydrothermal and low-temperature sedimentary uraninite (Frondel, 1958). Impurities in uraninite, such as Pb, Th, Ca, Y and lanthanides, can provide insight into the genesis of uraninite-fluid interactions and may also affect uraninite stability.

The U-mineralization was formed as a product of hydrothermal processes. It includes primary U-minerals with low Th-uraninite (ThO_2=3.15 %), while thorium contents of magmatic uraninite reach levels above approximately 10 or 12 wt. % ThO_2 (Frondel, 1958; Förster, 1999). It is obvious that for the generation of uranium mineralization, primary magmatic processes as well as post-magmatic, hydrothermal activity are important. The main magmatic differentiation process in peraluminous granites caused the progressive removal of poorly soluble minerals and thus corresponding enrichment of incompatible elements. In leucocratic facies, uranium is mainly located uraninite crystals (Friedrich et al., 1989). The whole rock uranium content increases with the evolution grade of the magma. Additional uranium enrichments are related to uraninite concentrations in post- magmatic shear zones associated with mineralogical evidence of an ortho-derived fluid phase rich in F, B, Li, Sn, Be, Zr, LREE and PO_4^{3+} (Friedrich et al., 1989). Therefore, uranium will be strongly held in the structure of refractory minerals and will not be easily leachable by hydrothermal solutions especially if they circulate shortly after magma emplacement and crystallization (Cuney & Friedrich, 1987).

Conclusions

1 – Mineralization In the shear zone includes primary uranium uraninite with low- Th content, which indicates the mineral was formed by post-magmatic hydrothermal processes, along with minerals such as ferrocolumbite, fergusonite, uraninite, galena and hematite. Hydrothermal uraninite commonly contains low Th and REE, whereas these elements are largely absent from hydrothermal and low-temperature sedimentary uraninite (Frondel, 1958). According to Romberger (1984), U is transported in the hydrothermal solutions in the uranyl state and precipitation of U would occur, if the physicochemical conditions of the solutions changed through reduction and an increase of pH. Increase in pH can be produced by loss of acid volatile components or reaction with host feldspars. There must be a reservoir of available electrons to allow this reduction to occur. Sources of exchangeable electrons in natural systems may be Fe^{2+} or organic material in wall rocks.

2 – The presence of galena is very good evidence for hydrothermal fluids. Therefore, the hydrothermal origin could be accepted for mineralizations within the shear zone associated with

quartz veins rich in gold, silver, bismuth and Bi-Ni in chalcopyrite.

3 – The altered granites of the Hangaliya shear zone are enriched in Au, Ag, Bi, Co and Ni with chalcopyrite, which suggests circulation of these metals from serpentinites due to the felsic intrusion (Nugrus granite). All of the gold in this assemblage was precipitated prior to sulphides, since native gold grains are visible within the pyrite, or in the chalcopyrite as inclusions. Nickel (Ni-Bi) is hosted mostly by chalcopyrite. The remainder of Ni-Bi precipitated from a hydrothermal fluid during metamorphism and enriched the products of the latest paragenesis.

4 – The U-mineralization was formed as product of hydrothermal processes. It includes primary U-minerals (uraninite with low Th content) and zircon minerals, with fluorite inclusions confirming their hydrothermal origin (i.e. low Th contents of hydrothermal uraninite).

References

Abdel Tawab, M. M. 1992: Gold exploration in Egypt from Pharaonic to modern times. Zentralbl. Geol. Paläont. Teil 1: 2721-2733.

Almond, D. C., Ahmed, F. & Shaddad, M. Z. 1984: Setting of gold mineralisations in the northern Red Sea hills of Sudan. Econ. Geol. 79: 389-392.

Azer, N. 1966: Remarks on the origin of Precambrian mineral deposits in Egypt (U.A.R.). Mineral Petrol. 11/1-2: 41-64.

Botros, N. S. 2004: A new classification of the gold deposits of Egypt. Ore Geol. Rev. 25: 1-37.

Cepedal, A., Fuente, M. F., Izard, A. M., Nistal, S. G. & Barrero, M. 2008: Gold-bearing As-rich pyrite and arsenopyrite from the El Valle gold deposit, Asturias, Northwestern Spain. The Canadian Mineralogist 46/1: 233-247.

Cuney, M. & Friedrich, M. 1987: Physicochemical and crystal-chemical controls on accessory mineral paragenesis in granitoids: implications for uranium metallogenesis. Soc. fran. Minéral. Cristallog. Bull. 110/2-3: 235-248.

El-Gaby, S., List, F. K. & Tehrani, R. 1988: Geology, evolution and metallogenesis of the Pan African belt in Egypt. In: El-Gaby, S. & Greiling, R. O. (eds.): The Pan African belt of north east Africa and adjacent areas. Braun Schweig (Vieweg): 17-68.

El-Husseiny, M. O., Ali, M. A. & Roz, M. E. 2006: The Late Pan-African dykes within Nugrus granite, South Eastern Desert, Egypt: mineralogical and radiometrical constrains. Proc. 4th International symposium on Geophsics, Tanta Univ.: 340-349.

El Ramely, M. F., Ivanov, S. S. & Kochin, G. C. 1970: The occurrence of gold in the Eastern Desert of Egypt. Studies on some mineral deposits of Egypt. Part I, Sec. A. metallic minerals. Geol. Surv. Egypt. 21: 1-22.

El Shazly, E. M. 1957: Classification of Egyptian mineral deposits. Egypt. J. Geol. 1: 1-20.

Garson, M. S. & Shalaby, I. M. 1976: Pre-Cambrian-Lower Paleozoic plate tectonics and metallogenesis in the Red Sea region. Spec. Pap. Geol. Assoc. Can. 14: 573-596.

Förster, H. J. 1999: The chemical composition of uraninite in variscan granites of the Erzgebirge, Germany. Mineralogical Magazine 63: 239-252.

Friedrich, M. H., Cuney, M., & Cregu, G. 1989: Uranium geochemistry in peraluminous leucogranites, A conference Report. Uranium 3: 353-385.

Frondel, C. 1958: Systematic mineralogy of uranium and thorium. U. S. Geological Survey Bulletin: 1064-1400.

Hassaan, M. M. & El-Mezayen, A. M. 1995: Genesis of gold mineralization in Eastern Desert, Egypt. Al-Azhar Bull. Sci. 6: 921-939.

Harraz, H. Z. 2000: A genetic model for a mesothermal Au deposit: evidence from fluid inclusions and stable isotopic studies at El Sid Gold Mine, Eastern Desert Egypt. J. Afr. Earth Sci. 30: 267-282.

Harraz, H. Z. 2002: Fluid inclusions in the mesothermal gold deposit at Atud mine: evidence from fluid inclusions and stable isotopic studies at El Sid Gold Mine, Eastern Desert Egypt. J. Afr. Earth Sci. 35: 347-363.

Hume, W. F. 1937: The minerals of economic value associated with the intrusive Precambrian igneous rocks. Geology of Egypt. Geological Survey of Egypt 3: 689-990.

Hussein, A. A. 1990: Mineral deposits. In: Said, R. (ed.): The geology of Egypt, Balkema-Rotterdam, Rockfeild: 511-566.

Khalil, K. I. & Helba, H. A. 1998: Gold mineralization and its alteration zones at Hangaliya gold mine, Eastern Desert Egypt. The 10th Ann. Meet. Mineral. Soc. Egypt. 4 (Abstract).

Klemm, D., Klemm, R. & Murr, A. 2001: Gold of the Pharaohs-6000 years of the gold mining in Egypt and Nubia. J. Afr. Earth. Sci. 33: 643-659.

McMillan, R. H. 1978: Genetic aspects and classification of important Canadian uranium deposits. In: Kimberly, M. M. (ed.): Uranium deposits: Their mineralogy and origin. Mineral. Assoc. Can. Short course Handbook 3: 187-204.

Osman, A. 1989: Distribution of gold among quartz, sulfides and oxides in the Hangaliya gold mine, Eastern Desert Egypt. M.E.R.C., Earth Sci. Series, Ain Shams Univ. 3: 168-178.

Osman, A. & Dardir, A. 1986: On the gold-bearing rocks and alteration zones at Hangaliya gold mine, Eastern Desert Egypt. The 5th Symp. Precamb. Develop., Cairo (Abstract).

Osman, A. & Dardir, A. 1989: On the mineralogy and geochemistry of some gold-bearing quartz vein in the Central Eastern Desert of Egypt and their wallrocks. Annals Geol. Surv. Egypt. 15: 17-25.

Paktunc, D., Kingston, D. & Pratt, A. 2006: Distribution of gold in pyrite and in products of its transformation resulting from roasting of refractory gold ore. The Canadian Mineralogist 44: 213-227.

PALENIK, C. S., UTSONOMIYA, S., REICH, M. KESLER, S. E., WANG, L. & EWING, R. C. 2004: "Invisible" gold revealed: direct imaging of gold nanoparticles in a Carlin-type deposits. American Mineralogist 89: 1359-1366.

REICH, M., KESLER, S. E., UTSONOMIYA, S., PALENIK, C. S. & EWING, R. C. 2005: Solubility of gold in arsenian pyrite. Geochim. et Cosmochim. Acta 69: 2781-2796.

ROMBERGER, S. B. 1984: Transport and deposition of uranium in hydrothermal systems at temperatures up to 300 °C: geological implications. In: DEVIVO, B., IPPOLITO, F., CAPALDI, G. & SIMPSON, P. R. (eds.): Uranium geochemistry and resources. Inst. Min. Metall.: 12-17.

SABET, A. H. & BORDONOSOV, V. P. 1984: The gold ore formations in the Eastern Desert of Egypt. Ann. Geol. Surv. Egypt 16: 35-42.

SIMON, G., HIANG, H., PENNER-HAHN, J. E., KESLER, S. E. & KAO, L. 1999: Oxidation state of gold and arsenic in gold-bearing arsenian pyrite. American Mineralogist 84: 1071-1079.

SOLIMAN, M. M. 1986: Ancient emerald mines and beryllium mineralization associated with Precambrian stanniferous granites in the Nugrus-Zabara area, southeastern Desert, Egypt. Arab J. Sci. Res. 4/2: 529-548.

SUROUR, A. A., ATTAWIYA, M. Y., HUSSEIN, H. A. & EL-FEKY, M. G. 1999: Shear zone microfabrics and multiple source of gold at the Hangaliya gold mine, Eastern Desert, Egypt. Egyp. Jour. Geol. 43/1: 29-44.

SUROUR, A. A., EL-BAYOUMI, R. M., ATTAWIYA, M. Y. & EL-FEKY, M. G. 2001: Geochemistry of wall rock alterations and radioactive mineralization in the vicinity of Hangaliya uraniferous shear zone, Eastern Desert, Egypt. Egyp. Jour. Geol. 45/1: 187-212.

TAKLA, M. A. 2001: Gold mineralization in Egypt – An overview. The Mineralogical Society of Egypt. The 14th Annual Meeting 3 (Abstract).